Journal of Medicinal and Chemical Sciences 6 (2023) 710-719

Journal of Medicinal and Chemical Sciences

Journal homepage: http://www.jmchemsci.com/

Original Article

Biological Test of Porous Geopolymer as a Bone Substitute

Haifaa Abdul Ameer Radhi*, Maha Abdulaziz Ahmad

[1]*Department Periodontics, Colleg of Dentistry, University of Baghdad, Baghdad, Iraq*
[2]*Colleg of Dentistry, University of Baghdad, Periodontics Department, Baghdad, Iraq*

ARTICLE INFO

Article history

Receive: 2022-06-27
Received in revised: 2022-08-03
Accepted: 2022-10-14
Manuscript ID: JMCS-2209-1771
Checked for Plagiarism: **Yes**
Language Editor:
Dr. Fatimah Ramezani
Editor who approved publication:
Dr. Gholamabbas Chehardol

DOI:10.26655/JMCHEMSCI.2023.4.2

KEYWORDS

Metakaolin
Porous geopolymer
Bone substitute
In vivo
Foaming agent and stabilizing agents

ABSTRACT

Bone substitute materials in the current use sustain several drawbacks such as donor site morbidity, induce immunity, availability, and economic production. New synthetic bone substitutes are needed that overcome these drawbacks. This study aimed to produce a porous geopolymer and evaluate its usefulness as a bone substitute. Metakaolin-based geopolymer with different porosity percentages and sizes was produced by the addition of hydrogen peroxide and olive oil in different ratios to the geopolymer paste. Image J analysis had used to calculate the porosity percentage and size. Geopolymers with the highest porosity percentage and size range were selected for *in vivo* testing on animals. In the *in vivo* study, porous geopolymer was implanted in femur bones of 12 rabbits. The right femur of each rabbit served as the positive control (using the commercial bone replacement TEEBON®), and the negative control group received no treatment. The left femur was used to implant the geopolymer. Two and four weeks after implantation, biopsies were performed for histological analysis. After two and four weeks, a histological examination of the implanted material revealed the development of bone trabeculae with minimal inflammation. As compared with commercial bone substitutes, geopolymers improved bone formation. Owing to the results, porous geopolymers could be the promising materials for bone substitutes, as they are available and cost effective.

GRAPHICAL ABSTRACT

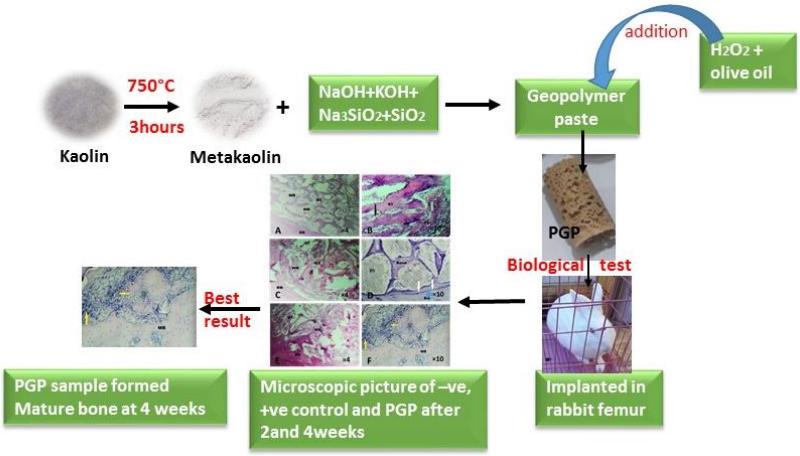

* Corresponding author: Haifaa AbdulAmeer Radhi
✉ E-mail: Email: haifa.ghaib1904@codental.uobaghdad.edu.iq

Introduction

Alveolar bone loss is still one of the drastic problems in dentistry that complicates the survival and aesthetics of natural teeth, dental implants, and other prosthodontic replacements [1].

The significant alveolar bony defect needs bone grafting procedure that either autografting, synthetic bone graft, or substitute [2]. Autograft has its limitation as it undergoes fast resorption and donor site distress [3]. Encouraging biomaterial advancement as bone substitutes had accomplished by understanding materials element behaviors, surface properties, and interaction with the biological environment to ensure its safety and bioactivity [4]. The synthetic bone may be a polymer, ceramic, or composite material [5]. The aim of most researchers is the investment of inexpensive and naturally available materials. Geopolymer is an inorganic polymer with typical ceramic behavior that has been developed as an industrial material to substitute Portland cement. Geopolymer formation has occurred from polymerization between alkaline activated materials and aluminum silicate source materials [6]. The good mechanical and physical properties of geopolymer encourage its studies as biomaterials, such as vehicles for drug delivery [7, 8] and bone substitutes [9-11].

The production of porous geopolymer could be in several ways like foaming agent addition, the addition of lost fillers, and 3D printing technique [12, 13]. Porous geopolymer is used for acoustic isolations, thermal isolations, and water purification [14]. Due to its heterogeneous macro- and micro-porosity gives the appearance of bone tissue [15].

Porous geopolymer influence on tissue response had proved through an *in vivo* study, as animal studies are an effective way to give a close picture of the material behavior in the human body [16].

This study used metakaolin-based geopolymer, a preferred source for biomaterial [17]. It was modified by foaming agents to produce porous geopolymer for its implementation as a bone substitute.

Materials and Methods

Production of metakaolin

Iraq's western desert kaolin (Dwaikhla) was heated at 750 °C for three hours in a nonvacuum digital muffle furnace [Model (MF-12) 1200 °C HYSC/KORIA] to transform to metakaolin and fabricate a geopolymer based on metakaolin [18].

Material characterization

Kaolin, metakaolin powders, and geopolymer materials had characterized by the estimation of the mineral phase by "X-ray diffraction" (XRD 6000, Shimadzu, Japan). Atomic Absorption device (Varian, America) was used for chemical analysis of kaolin and metakaolin powder. Field emission-scanning electron microscopy (FE-SEM) (inspect f50 FE-SEM; Netherland) with an accelerating voltage of 30 kV was used for the surface characterization of the geopolymer sample with a larger pore size and percentage.

Geopolymer preparation

The adopted geopolymer chemical formulation was (0.5K.0.5Na. $1Al_2O_3$. 3.8 SiO_2. 9ml of H_2O). Likewise, the alkaline silicate to alkaline hydroxide ratio was kept at 3.02 [19].

The alkaline activator solution had prepared by dissolving 2.245 g of potassium hydroxide pellets (KOH) (Thomas Baker, India) and 0.754 g of sodium hydroxide pellets (NaOH) (Thomas Baker, India) in 9 ml distilled water in a 50 mL size beaker. When the hydroxide salts pellet had dissolved quietly in the water, 2.318 g of sodium silicate (Na_2SiO_3) (Thomas Baker, India) was added to the mix on a magnetic shaker, and then the stirrer temperature was raised to 70-80 °C at a low speed. After the dissolution of all silicate salts, 2.931 g of amorphous silica (Thomas Baker, India) was added to the solution.

When all silica dissolved entirely in about an hour, the desired water volume had added to compensate for the vaporized water lost during heating. Then, the solution was left to cool at room temperature. Next, 10.730 g of metakaolin powder had added to the mixture and it had mixed at a set pace with an electric overhead mixer (1000 rpm) for 10 minutes [19]. The added concentration of

olive oil (cooking oil Zeer, Turkey) (3% and 4% wt/wt) is related to the wet geopolymer slurry. After that, the resulting geopolymer paste was divided into two groups (A and B) pastes. Each group had subdivided into three groups concerning the addition of hydrogen peroxide (H_2O_2) (30%W/V, India) at concentrations of (3%, 4%, and 4.5%) wt/wt of the geopolymer wet slurry, as shown in Table 1.

Preparation of porous geopolymer PGP

The prepared geopolymer paste was kept for one and a half hour to improve the viscosity. The olive oil and hydrogen peroxide were added to the mix and were mixed using an electric mixer for 1 min at a speed of 1000 rpm. The yielded paste was poured into a polyvinyl chloride cylindrical mold with dimensions of 15 × 30 mm diameter and length, respectively. Half of the mold was filled with the paste to allow for the foam expansion to fill the entire mold (20). Then, the paste was kept to set for 24 hours at room temperature. The dried porous geopolymer was demolded and prepared to estimate the sizes and percentages of its pores.

Estimation of pores sizes and percentage

The PGP sample with a higher porosity and the optimum pore size had been selected by capturing ten photos for each PGP sample via optical microscopy (Nikon Eclipse ME 600, Japan) [21]. The "Image J" program was utilized to determine the percentage and pore size [22].

Laboratory animals

Twelve white male New Zealand rabbits weighing approximately 2 and 2.5 kg were employed in this study and kept in the animal house of the (National Center for Drug Control and Research/Iraq) at a steady humidity and 23 °C according to the National Council guide for animal care in laboratories sanctioned by the Animal Ethics Committee of the College of Dentistry of Baghdad University. According to the ethical acceptance with project no. 269621 on 25/3/2021.

The animals were kept in special cages for about one week before surgery for adaptation. The PGP and TEEBONE® (the commercial bone substitute) had implanted in the rabbits. The experimental animals had divided into two groups (2 and 4 weeks), each of which included six animals euthanized for the histological analysis.

Surgical implantation

The rabbits were injected with an anesthetic solution composed of 1 mL/kg ketamine hydrochloride 10% (30 mg/kg) and 0.1 mL xylazine (5 mg/kg). Under aseptic conditions, the femoral bone of both legs in each rabbit was accessed by a lateral incision in the skin, fascia, and periosteum. Bone holes were created by a round bur of 2 mm diameter at 1000 rpm speed, accompanied by saline coolant irrigation [23]. The resulted were three holes; two holes in the right femur and one in the left femur of each animal. Each hole had measured 2 × 2 mm in width and depth, respectively. Two holes in the right femur had been used for controls (the positive control hole had been filled with TEEBONE® while the negative control hole had been left without intervention). TEEBONE® is a biphasic bone graft composed of 25% tricalcium phosphate and 75% hydroxyapatite (Medibrex, Spain). The third hole in the left femur had filled with PGP to investigate the tissue response. The incision was sutured layer by layer using an absorbable catgut suture for the fascia and 3/0 black silk for the skin. At the end of each testing period (2 and 4 weeks), the rabbits were sacrificed with an overdose of anesthesia and injected intravenously.

Table 1: The combination of olive oil and hydrogen peroxide addition to geopolymer paste

Groups	A			B		
	A1	A2	A3	B1	B2	B3
Olive Oil by weight %	3%	3%	3%	4%	4%	4%
H_2O_2 wt%	3.5%	4%	4.5%	3.5%	4%	4.5%

Both femoral bones were excised, and the soft tissue was cleaned, and placed in formalin with a concentration of 10% for fixation to prepare for the histological examination. The fixated bone blokes by formalin were demineralized with 10% formic acid, deeply seated in paraffin, and longitudinally sectioned about 5 µ in thickness. Hematoxylin and eosin had been used to stain the sections before examination using an optical microscope. Three slides had obtained from each test block. Three histological sections were analyzed for each animal. The histological changes and histomorphometric analysis were evaluated under a light microscope (with objective lens 4 X, 10 X, and 40 X) [24]. After that, the slices had photographed by a camera (Olympus-Japan). New bone deposition percentage, cell count of osteoblast, osteocyte, progenitor cells, fibroblast, and inflammatory cells were quantified by the histomorphometric analysis.

Data analysis

The obtained data were examined using statistics (One-way ANOVA) for the multiple comparisons with Graph Pad Prism 8. The values had presented as the mean and standard deviation (SD) of triplicate measurements, and p-value = 0.0001 indicated a significant level.

Results and Discussion

Chemical analysis

Table 2 demonstrates the chemical analysis of both kaolin and metakaolin. The percentage of the chemical composition of the kaolin, which was metal oxides was less than their analog in metakaolin. Metakaolin used in this study had obtained from kaolin calcination. The chemical analysis of both of them ensures the transformation process of kaolin to metakaolin after heat application. The element analysis for metakaolin had used in the stoichiometric calculation of the final geopolymer formula.

Table 2: Kaolin and metakaolin chemical ingredient

Elements %	SiO_2 %	Al_2O_3 %	Na_2O %	K_2O %	Fe_2O_3 %	TiO_2 %	CaO %	MgO %	SO_3 %	LOI %
Metakaolin	54.48	38.73	0.01	0.33	1.58	0.89	0.56	0.31	<0.07	0.73
Kaolin	49.39	34.3	0.014	0.3	0.76	0.51	0.28	0.16	<0.07	12.18

X-ray diffraction

The XRD pattern in Figure 1**a** for kaolin showed clear peaks representing the crystalline structure disappeared in the metakaolin Figure 1**b**, due to the dehydroxylation process at 750 °C for 3 hours [19]. The higher curve at 26° was corresponded to intensities of 208, 338, and 166 for kaolin, metakaolin, and geopolymer, respectively. This peak represents crystalline quartz. The second strong peak 25° represents the kaolinite crystal gives intensity 434, 73, and 46 for kaolin, metakaolin, and geopolymer, as presented in Figure 1**c**. It had a high intensity in kaolin. However, it had reduced in metakoalin as a result of heat application. Likewise, it had further decreased in the geopolymer. The metakaolin had dissolved in an alkaline activator during the polymerization process that indicates the mineral phase transformation of kaolin [26, 27].

Estimation of pore size and percentage

The average pore size and the proportion of porous geopolymer samples are indicated in Table 3. While, the B3 group had a large pore size and percentage value, the other groups had the approximate values.

Geopolymer was transformed into a porous material by the addition of H_2O_2 and Olive oil as foaming agents. H_2O_2 as a blowing agent did not interfere with alkaline activation reaction without residuals [28]. The olive oil (vegetable oil) had been used as a surfactant due to its low price and accessibility [14]. The B3 group had the highest pore percentage (46.89%) and the largest range of pore sizes (3.23-735.285). It was reported that increasing the hydrogen peroxide concentration produces large pores [29, 30] which is why stabilizing agents (such as surfactants like olive oil) had used. The surface tension of the gas/slurry system was decreased and the bubbles union was

ceased. The olive oil can also regulate pore size and dispersion [14, 30]. Vegetable oils that react with an extremely alkaline GP can contribute to the interconnected porous network [31].

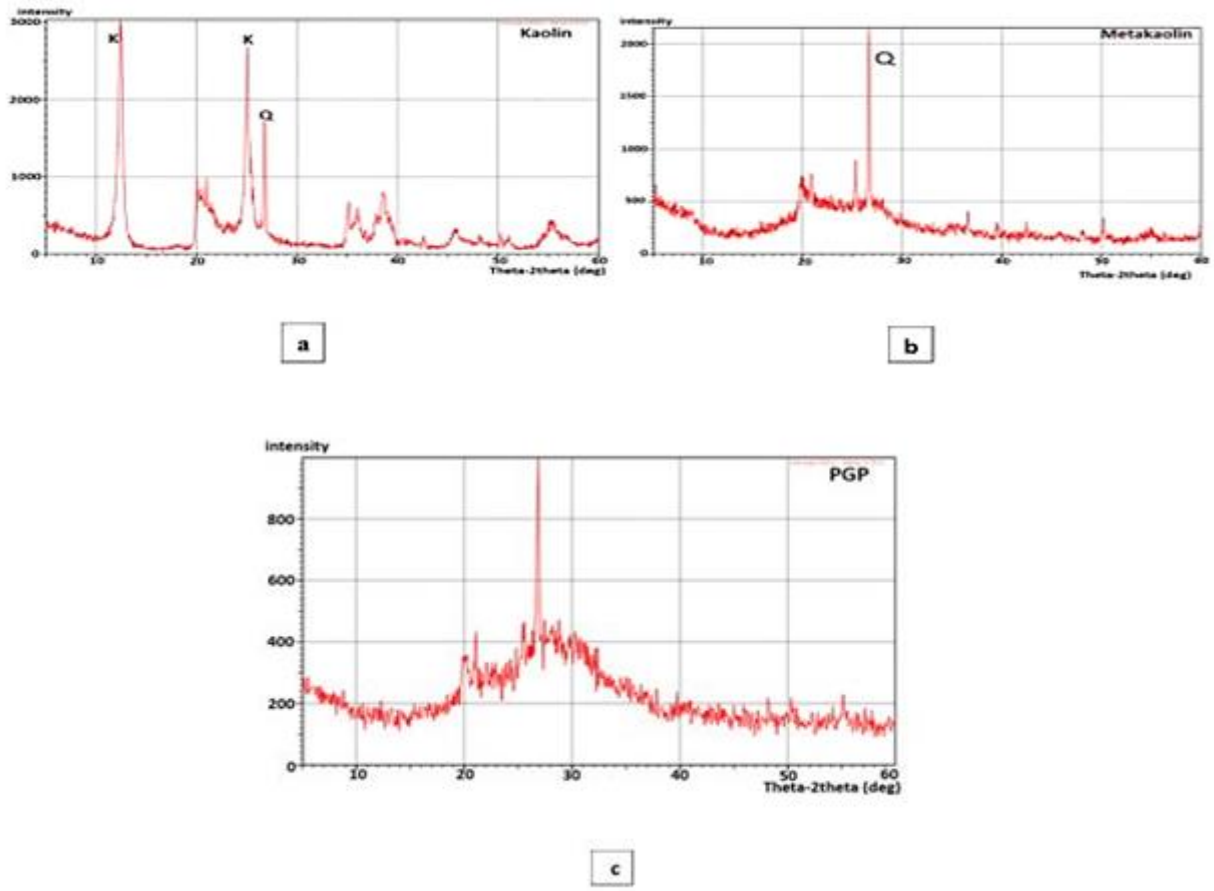

Figure 1: The XRD pattern for (a) kaolin, (b) metakaolin, and (c) porous geopolymer

Microstructural examination

The micrographs in Figure 2 show the morphology of the porous geopolymer sample symbolled as PGP with a greater pore size and percentage at different magnifications 20 x, 40 x, and 300 x. The pores ranging from 3-1000 µ appear interconnected with each other with a wide throat size. The reason for using porous materials as scaffolding materials with various pore sizes, shapes, and interconnections is to mimic human spongy bone that would allow vascularization, cell adhesion, differentiation, and increased bone cell growth [15].

Table 3: Values of porosity percentage and size of porous geopolymer

Groups	Mean porosity Vol%	Mean of the pore size	
		The minimum µm	The maximum µm
A			
A1	38.70	3.20	386.47
A2	39.62	3.24	626.5
A3	38.19	3.23	707.68
B			
B1	37.05	3.24	643.42
B2	37.78	3.25	558.014
B3	46.89	3.23	735.285

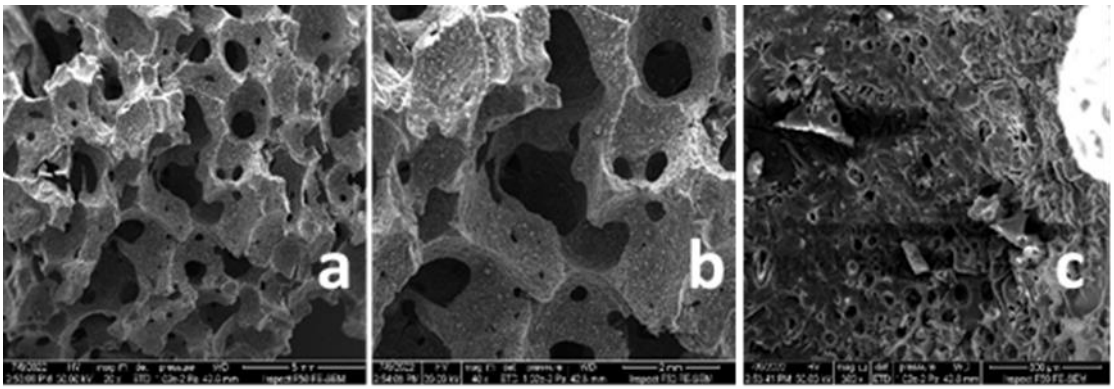

Figure 2: FE-SEM indicates the microstructural characteristic of the PGP sample. (a) 20 x, (b) 40 x, and (c) 300 x magnification

Histological observations

The prepared porous geopolymer was implanted to investigate its biocompatibility and bioactivity in bone formation

All samples from a negative control group at two weeks postoperatively show many bone trabeculae encircled by the bone marrow. The woven bone is characterized by the irregular arrangement of collagen fibers with the osteogenic cells scattered between them. Osteoblast and osteocyte can detect. Four weeks after surgery, the samples show that the fibrous tissue had filled the whole space, and the bone trabeculae had coalesced with the basal bone, as revealed Figure 3A and B.

Two weeks after surgery, a microscopic examination of all specimens from a positive control group. The revealed woven bones with dispersed bone trabeculae had been encircled by osteoblastic cells. In addition, the osteogenic progenitor cells had displayed in Figure 3C. The samples reveal that the bone trabeculae unite with the basal bone in some areas and had surrounded bone substitute material (TEEBONE®) 4 weeks after surgery, as illustrated in Figure 3D. The histological examination of PGP test group was done at two weeks. The bone trabeculae coalesce with the basal bone. The woven bone and osteoid tissue with a high number of progenitor cells were present. At four weeks, the mature bone was visible in all specimens and filled the opening with more proliferating cells, as illustrated in Figure 3E and F.

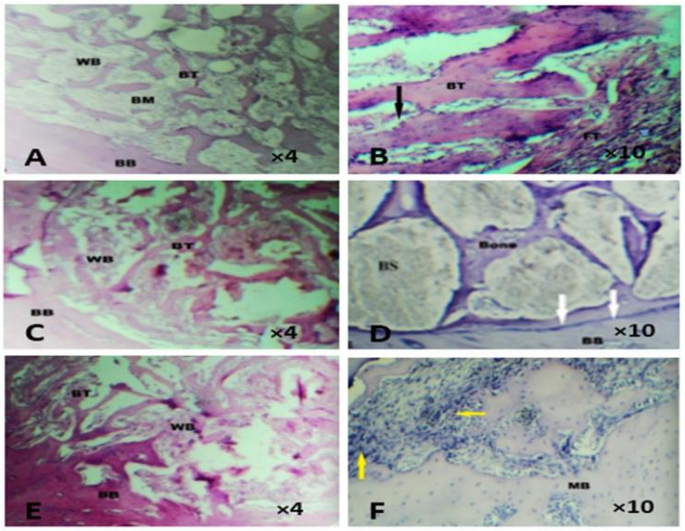

Figure 3: Microscopic pictures of various materials examined at (2 and 4 weeks) show basal bone (BB) and a few sparsely distributed bone trabeculae (BT), woven bone (WB), bone substitute (BS), osteoblast (black arrow), proliferating progenitor cells (yellow arrows), reversal line (white arrows), and fibrous tissue (FT)

Statistical findings

Table 4 indicates the highest mean value of osteoblast cells (Ob) count was 10.17 ± and SD was 1.169 in porous geopolymer group (PGP), followed by progenitor cell (Pc) count mean value, and SD were 9.5± 0.548 for the same group at two weeks period. While, the highest mean value in four weeks period is for (Pc) mean value of 17.33±1.506 for the PGP test group followed by (Ob) cell average value and SD were 7.333 ± 0.817, and then the (Oc) cell average value and SD were 6.83±0.753 as revealed in Figure 3. Table 5 presents p-value (0.0001) of the bone cells (Ob), (Pc), and (Oc) between (PGP) and the other conrol groups after 2- and 4-weeks duration. The significant differences are present for the fibroblast cells between the control groups (positive and negative) and between the PGP group versus positive control group over four weeks. The progenitor cell (Pc) shows a significant difference between negative control versus positive control over two weeks. The mean values of the inflammatory cell count (Inf) showed the non-significant differences between the experimental groups in 2 and 4 weeks, as revealed in Figure 4.

Table 4: The descriptive statistic of bone cells for all experimental groups after 2 and 4 weeks

Interval	Cell types	Experimental Groups					
		-ve		+ve		PGP	
		Mean	SD	mean	SD	mean	SD
2 weeks	Ob*	2.167	0.753	4.167	0.753	10.17	1.169
	Pc*	4.167	0.753	2.167	0.408	9.500	0.548
	Oc*	1.667	0.517	1.667	0.517	6. 167	0.753
	Fb*	1.333	0.516	1.500	0.548	1. 333	0.817
	Inf*	3.000	0.633	3.500	0.548	4. 167	0.983
4 Weeks	Ob	4.167	0.7528	4.167	0.753	7.333	0.817
	Pc	2.333	0.5164	2.167	0.408	17.33	1.506
	Oc	3.167	0.4082	4.167	0.753	6.833	0.753
	Fb	5.500	0.5477	3.333	0.516	1.833	0.408
	Inf	4.833	0.7528	3.333	0.516	2.833	0.753

Ob=osteoblast, Pc*=progenitor cell, Oc*=osteocyte, Fb*=fibroblast, and Inf*=inflammatory cell.*

Table 5: Multiple comparisons of cellularity between every two groups after 2 and 4 weeks using one-way ANOVA

Interval	Groups	Osteoblast (p-value)	Progenitor (p-value)	Osteocyte (p-value)	Fibroblast (p-value)	Inflammatory (p-value)
2 Weeks	-ve vs. +ve	0.0064	<0.0001	>0.9999	.895	0.4928
	-ve vs. PGP	<0.0001	<0.0001	<0.0001	>.999	0.0603
	+ve vs. PGP	<0.0001	<0.0001	<0.0001	.895	0.2972
4 Weeks	-ve vs. +ve	>0.9999	0.9504	0.0769	<0.0001	0.0746
	-ve vs. PGP	<0.0001	<0.0001	<0.0001	<0.0001	0.0604
	+ve vs. PGP	<0.0001	<0.0001	<0.0001	0.0003	0.4339

Histological images among the experimental groups (negative and positive) controls and test group (PGP) were compared at two different healing intervals (2 and 4 weeks). The highest mean values of osteogenic cells and less inflammation related to the PGP group. This result may indicate the biocompatibility and bioactivity of the PGP material. These results are consistent with the previous *in vitro* and *in vivo* studies conducted on and (9-11) metakaolin-based geopolymers with different formulations, proved the hydroxyapatite formation.

Bone formation induced by PGP could be explained by the following scenarios:

Aluminum-silicate glass ceramic is made of silicon and aluminum forms a network. Like the main composition of PGP, a silica gel microsphere was produced by interacting with the simulated bodily

fluid (SBF), which underwent dissolution, network fragmentation, and silanol group development. The calcium and phosphorus ions move from the SBF to the glass microsphere. They start to form the building blocks of a physiologically active hydroxy carbonate apatite [32].

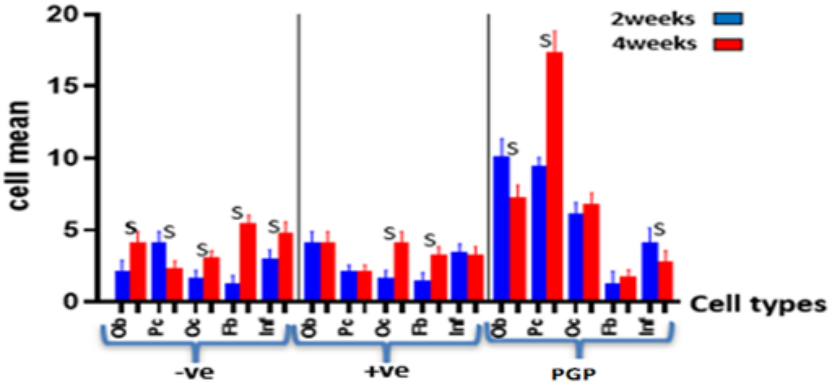

Figure 4: Bone cell mean values of the experimental groups at 2 and 4 weeks

The porous geopolymer had the same mineral phase as metakaolin, as proved by the XRD analysis. The chemical composition of metakaolin is closely similar to the bioactive bioglass ceramic material [33]. Accordingly, the cation exchange between the PGP surface and bodily fluid, which results in the creation of silanol groups (Si-OH) and silica gel, may explain how a new bone formed. Because there are more OH- ions in the solution as a result of this action, the solution alkalinity increased. Subsequently, amorphous phosphate, composed of calcium and phosphate, forms a top the silica-rich layer and spontaneously converts into hydroxyl-apatite [$Ca_{10}(PO_4)_6(OH)_2$] [33]. Hydroxyapatite is the inorganic mineral interspersed in a collagen matrix of normal bone. It explains the formation of trabecular bone after two weeks and the mature bone at four weeks of rabbit femur implantation.

Conclusion

With the limitation of this study, metakaolin-based PGP is possibly biocompatible and bioactive material, and also it could be a potential bone substitute inducing a negligible inflammatory response. PGP can induce a dense trabecular bone formation at two weeks of animal bone implantation and increase the amount of mature bone over time after four weeks. Such material needs further investigations for a wide defect, modification of the physical form, and over a long time to confirm the possible long-term bioactivity.

Acknowledgments

I would like to express my special thanks to Prof Dr. Zuhair Jabbar Abdul Ameer, College of Engineering, University of Karbalaa, Iraq and Prof Dr. Mohanad Mohsin Ahmed, College of Medicine, University of Karbalaa, Iraq for sharing their scientific remarks and incessant support throughout this research work.

Funding

This research did not receive any specific grant from funding agencies in the public, commercial, or not-for-profit sectors.

Authors' contributions

All authors contributed to data analysis, drafting, and revising of the paper and agreed to be responsible for all the aspects of this work.

Conflict of Interest

The anthers declared that they have no conflict of interest.

ORCID:

Haifaa AbdulAmeer Radhi
https://orcid.org/0000-0002-9961-8497

References

[1]. Könönen E., Gursoy M., Gursoy U.K., Periodontitis: a multifaceted disease of tooth-supporting tissues, *Journal of clinical medicine*,

2019, 8:1135 [Crossref], [Google Scholar], [Publisher]
[2]. Jonasson G., Skoglund I., Rythén M., The rise and fall of the alveolar process: Dependency of teeth and metabolic aspects, *Archives of oral biology*, 2018, **96**:195 [Crossref], [Google Scholar], [Publisher]
[3]. Luca R.E., Todea C.D., Duma V.F., Bradu A., Podoleanu A.G., Quantitative assessment of rat bone regeneration using complex master-slave optical coherence tomography, *Quantitative Imaging in Medicine and Surgery*, 2019, **9**:782 [Crossref], [Google Scholar], [Publisher]
[4]. Baldwin P., Li D.J., Auston D.A., Mir H.S., Yoon R.S., Koval K.J., Autograft, allograft, and bone graft substitutes: clinical evidence and indications for use in the setting of orthopaedic trauma surgery, *Journal of orthopaedic trauma*, 2019, **33**:203 [Crossref], [Google Scholar], [Publisher]
[5]. Kumar P., Vinitha B., Fathima G., Bone grafts in dentistry, *Journal of pharmacy & bioallied sciences*, 2013, **5**:125 [Crossref], [Google Scholar], [Publisher]
[6]. Amritphale S.S., Bhardwaj P., Gupta R., Advanced Geopolymerization Technology, in Geopolymers and Other Geosynthetics, *IntechOpen*, 2019 [Crossref], [Google Scholar], [Publisher]
[7]. Forsgren J., Pedersen C., Strømme M., Engqvist H., Synthetic geopolymers for controlled delivery of oxycodone: adjustable and nanostructured porosity enables tunable and sustained drug release, *PLoS One*, 2011, **6**:e17759 [Crossref], [Google Scholar], [Publisher]
[8]. Cai B., Engqvist H., Bredenberg S., Evaluation of the resistance of a geopolymer-based drug delivery system to tampering, *International Journal of Pharmaceutics*, 2014, **465**:169 [Crossref], [Google Scholar], [Publisher]
[9]. Oudadesse H., Derrien, A. C., Mami, M., Martin, S., Cathelineau, G., & Yahia, L.., Aluminosilicates and biphasic HA-TCP composites: studies of properties for bony filling, *Biomedical Materials*, 2007, **2**:S59 [Crossref], [Google Scholar], [Publisher]
[10]. Oudadesse H., Derrien A.C., Lefloch M., Davidovits J., MAS-NMR studies of geopolymers heat-treated for applications in biomaterials field, *Journal of materials science*, 2007, **42**:3092 [Crossref], [Google Scholar], [Publisher]
[11]. Catauro M., Bollino F., Papale F., Lamanna G., Investigation of the sample preparation and curing treatment effects on mechanical properties and bioactivity of silica rich metakaolin geopolymer, *Materials Science and Engineering: C*, 2014, **36**:20 [Crossref], [Google Scholar], [Publisher]
[12]. Bai C., Colombo P., High-porosity geopolymer membrane supports by peroxide route with the addition of egg white as surfactant, *Ceramics International*, 2017. **43**:2267 [Crossref], [Google Scholar], [Publisher]
[13]. Perumal P., Luukkonen T., Sreenivasan H., Kinnunen P., Illikainen M., *Porous alkali-activated materials*, in *New Materials in Civil Engineering*. 2020, 529-563 [Crossref], [Google Scholar], [Publisher]
[14]. Bai C., Colombo P., Processing, properties and applications of highly porous geopolymers: A review, *Ceramics International*, 2018, **44**:16103 [Crossref], [Google Scholar], [Publisher]
[15]. Faza Y., Harmaji A., Takarini V., Hasratiningsih Z., Cahyanto A., Synthesis of Porous Metakaolin Geopolymer as Bone Substitute Materials, in *Key Engineering Materials*, 2020, **829**:182, Trans Tech Publications Ltd., [Crossref], [Google Scholar], [Publisher]
[16]. Pound P., Ritskes-Hoitinga M., Can prospective systematic reviews of animal studies improve clinical translation?, *Journal of Translational Medicine*, 2020, **18**:15 [Crossref], [Google Scholar], [Publisher]
[17]. Pangdaeng S., Sata V., Aguiar J.B., Pacheco-Torgal F., Chindaprasirt P., Apatite formation on calcined kaolin–white Portland cement geopolymer, *Materials Science and Engineering: C*, 2015, **51**:1 [Crossref], [Google Scholar], [Publisher]
[18]. Rashad, A.M., Metakaolin as cementitious material: History, scours, production and composition–A comprehensive overview, *Construction and building materials*, 2013, **41**:303 [Crossref], [Google Scholar], [Publisher]
[19]. Al-dujaili A., Disher Al-hydary I.A., Zayer Hassan Z., Optimizing the Properties of Metakaolin-based (Na, K)-Geopolymer Using

Taguchi Design Method, *International Journal of Engineering*, 2020, **33**:631 [Crossref], [Google Scholar], [Publisher]
[20]. Lertcumfu N., Kaewapai K., Jaita P., Tunkasiri T., Sirisoonthorn S., Rujijanagul G., Effects of olive oil on physical and mechanical properties of ceramic waste-based geopolymer foam, *Journal of Reinforced Plastics and Composites*, 2020, **39**:111 [Crossref], [Google Scholar], [Publisher]
[21]. Bai C., Ni T., Wang Q., Li H., Colombo P., Porosity, mechanical and insulating properties of geopolymer foams using vegetable oil as the stabilizing agent, *Journal of the European Ceramic Society*, 2018, **38**:799 [Crossref], [Google Scholar], [Publisher]
[22]. Hajimohammadi A., Ngo T., Mendis P., Kashani A., van Deventer J.S., Alkali activated slag foams: the effect of the alkali reaction on foam characteristics, *Journal of cleaner production*, 2017, **147**:330 [Crossref], [Google Scholar], [Publisher]
[23]. Hanafy A., Hegab I., Effects of egg weight and light sources during incubation period on embryonic development and post-hatch growth of Japanese quail (Coturnix japonica), *European Poultry Science*, 2019, **83** [Crossref], [Google Scholar], [Publisher]
[24]. Slaets E., Naert I., Carmeliet G., Duyck J., Early cortical bone healing around loaded titanium implants: a histological study in the rabbit, *Clinical oral implants research*, 2009, **20**:126 [Crossref], [Google Scholar], [Publisher]
[25]. Ghelich P., Kazemzadeh-Narbat M., Hassani Najafabadi A., Samandari M., Memić A., Tamayol A., (Bio) manufactured Solutions for Treatment of Bone Defects with an Emphasis on US-FDA Regulatory Science Perspective, *Advanced NanoBiomed Research*, 2022, **2**:2100073 [Crossref], [Google Scholar], [Publisher]
[26]. El Alouani, M., S. Alehyen, and M.J.J.o.C. El Achouri, *Preparation, characterization, and application of metakaolin-based geopolymer for removal of methylene blue from aqueous solution, Journal of Chemistry*, 2019, **2019**:4212901 [Crossref], [Google Scholar], [Publisher]
[27]. Cao R., Fang Z., Jin M., Shang Y., *Study on the Activity of Metakaolin Produced by Traditional Rotary Kiln in China,* 2022, **12**:365 [Crossref], [Google Scholar], [Publisher]
[28]. Novais R.M., Ascensão G., Buruberri L.H., Senff L., Labrincha J.A., Influence of blowing agent on the fresh-and hardened-state properties of lightweight geopolymers, *Materials & Design*, 2016, **108**:551 [Crossref], [Google Scholar], [Publisher]
[29]. Şahin M., Erdoğan S.T., Bayer Ö., Production of lightweight aerated alkali-activated slag pastes using hydrogen peroxide, *Construction and Building Materials*, 2018, **181**:106 [Crossref], [Google Scholar], [Publisher]
[30]. Petlitckaia S., Poulesquen A., Design of lightweight metakaolin based geopolymer foamed with hydrogen peroxide, *Ceramics International*, 2019, **45**:1322 [Crossref], [Google Scholar], [Publisher]
[31]. Cilla M.S., Morelli M.R., Colombo P., Open cell geopolymer foams by a novel saponification/peroxide/gelcasting combined route, *Journal of the European Ceramic Society*, 2014, **34**:3133 [Crossref], [Google Scholar], [Publisher]
[32]. Todea M., Vanea E., Bran S., Berce P., Simon S., XPS analysis of aluminosilicate microspheres bioactivity tested in vitro, *Applied surface science*, 2013, **270**:777 [Crossref], [Google Scholar], [Publisher]
[33]. Ferraris S., Yamaguchi S., Barbani N., Cazzola M., Cristallini C., Miola M., Vernè E., Spriano S., Bioactive materials: In vitro investigation of different mechanisms of hydroxyapatite precipitation, *Acta biomaterialia*, 2020, **102**:468 [Crossref], [Google Scholar], [Publisher]

HOW TO CITE THIS ARTICLE
Haifaa AbdulAmeer Radhi, Maha Abdulaziz Ahmad. Design, Biological Test of Porous Geopolymer as a Bone Substitute. *J. Med. Chem. Sci.*, 2023, 6(4) 710-719
https://doi.org/10.26655/JMCHEMSCI.2023.4.2
URL: http://www.jmchemsci.com/article_159348.html